Desalination and Water Treatment
www.deswater.com

doi: 10.5004/dwt.2020.25118

181 (2020) 422–435
March

Toxic yellow cow dung powder (Auramine O dye) removal via *Ipomoea aquatica* waste

Y.C. Lu[a], N. Priyantha[b,c], Linda B.L. Lim[a,*], M. Suklueng[d]

[a]*Chemical Sciences Programme, Faculty of Science, Universiti Brunei Darussalam, Negara Brunei Darussalam, email: linda.lim@ubd.edu.bn (L.B.L. Lim), Tel. 00-673-8748010; email: yiechen_93@hotmail.com (Y.C. Lu)*
[b]*Department of Chemistry, Faculty of Science, University of Peradeniya, Sri Lanka*
[c]*Postgraduate Institute of Science, University of Peradeniya, Peradeniya, Sri Lanka, email: namal.priyantha@yahoo.com*
[d]*PSU Energy System Research Institute, Prince of Songkla University, Thailand, email: akemontri@gmail.com*

Received 26 May 2019; Accepted 2 November 2019

ABSTRACT

Ipomoea aquatica (water spinach), a popular local vegetable, was investigated for its remediation ability as a newly reported adsorbent to remove Auramine O dye from simulated aqueous solution. The adsorbent–adsorbate system reached equilibrium within a short period of 30 min. Adsorption was found to be exothermic, spontaneous and favourable. Modelling of the adsorption isotherm data with five isotherm models indicated that the Sips model was the most appropriate, giving a maximum adsorption capacity of 303.8 mg g^{-1}. Time-dependent experiments indicated that adsorption followed the pseudo-second order kinetics with a rate constant of 36.32 g $mmol^{-1}$ min^{-1}. No prominent reduction of dye removal was observed at different pH, showing the adsorbent's resilience to changes in medium pH. Results from this study clearly showed the potential of *Ipomoea aquatica* waste being utilized as a new low-cost adsorbent, given its high adsorption capacity when compared with many adsorbents, fast adsorption time and its ability to retain high adsorption capacity for many consecutive cycles when regenerated with base.

Keywords: Ipomoea aquatica; Basic Auramine O dye; Adsorption isotherm; Kinetic studies; Regeneration

1. Introduction

As a result of increasing industrial development, the amount of pollutants, such as heavy metals and synthetic dyes, being discharged into rivers, lakes and the oceans is constantly on the rise. Water being the "universal solvent" has the ability to dissolve many chemicals being dumped into the environment. The wastewater, if remains untreated, causes water pollution which in turn disrupts the ecosystem resulting in detrimental effects on aquatic lives. Not only can it result in shortening of the life span of these aquatic lives but also it can affect their reproduction. Accumulation of toxins in these aquatic lives makes their way up the food chain and thereby poses potential adverse health problems to human who consumes these aquatic animals. Further, drinking contaminated water can jeopardize our lives, as was clearly demonstrated by the occurrence of Arsenic poisoning in Bangladesh. Therefore, there is an urgent need to treat the wastewater prior to being discharged from its source of generation into the lakes, rivers or the ocean. One of the treatment methods is by adsorption technique whereby low-cost adsorbents such as industrial wastes [1], leaves [2], agro-wastes [3–5], fruit peels [6–9], synthesized materials [10] and others [11–13] have been shown to remove synthetic dyes and heavy metals. This method is simple and easy to carry out, and most importantly, it is low cost and effective.

Auramine O (AO) dye is a diarylmethane dye with two aromatic rings as shown in Fig. 1. It is a toxic yellow dye

* Corresponding author.

which fluoresces and is used as a colouring agent in textile and paper industries [14]. AO was chosen as the model dye in this study as it is widely used in India and is known as "Yellow Cow Dung powder" because the Indian people mix it with cow dung using bare hands as a decorative mixture for the front of their houses for auspicious events. As a result, the dye is adsorbed through the skin and causes staining and yellow discolouration, vomiting and nausea [15,16]. Being highly lethal and toxic, with lethal dose being 0.5 mg kg^{-1} body weight, AO has caused thousands of death in India and has been reported to cause poisoning to both children and adults alike [17,18]. AO is cheap and readily available, and there were many cases where AO was being taken as a suicidal drug. Studies have also shown that AO is carcinogenic and has the potential to cause liver and bladder cancer in both humans and rats [19,20]. It is also a neuro toxic poison that affects the central nervous system. AO is one of the ingredients used in the manufacture of incense as a colourant. When burnt, being thermo-stable, AO is released into the air, and a study by Tung et al. [21] shows that it promotes lung cancer malignancy.

This study investigates the use of waste derived from a popular vegetable in South East Asia known as *Ipomoea aquatica* (water spinach), locally known as "Kangkong". *Ipomoea aquatica* belongs to the Convolvulaceae family and is high in minerals, especially potassium and iron, and is a good source of fiber, Vitamin A and other nutrients [22,23]. It is readily available throughout the year, either cultivated or found growing in marshes and fields. In Brunei Darussalam, this is sold as a cheap vegetable in the open markets and is often stir-fried with a locally made fermented prawn paste known as "Belacan". Only the leaves and tender top part of the vegetable are eaten while majority of the stalk, which is less tender, is thrown away as waste. Hence in this study, the Kangkong stalk (KS) was used as the adsorbent to remove AO dye.

Ipomoea aquatica has been used in phytoremediation of heavy metals such as Cr(VI) [24], Pb(II) [25] and Cr(III) [26]. However, to date, the use of *Ipomoea aquatica* has not been reported as an adsorbent for the removal of pollutants. Hence, to the best of our knowledge, this is the first report to provide insight into the potential use of KS in wastewater remediation. In this study, we made use of the stalks that are being thrown away to evaluate its potential as a low-cost adsorbent to adsorb AO dye from simulated wastewater. Further, investigation into the possibility of regenerating and reusing the spent adsorbent will be reported.

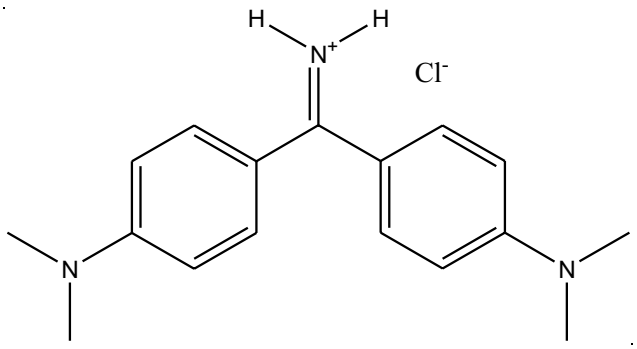

Fig. 1. Chemical structure of Auramine O dye.

2. Methods and materials

Ipomoea aquatica (water spinach) was purchased from the local open market in the Brunei-Muara District of Brunei Darussalam. The inedible stalks of *Ipomoea aquatica* (KS) were separated from the edible parts and washed several times with distilled water to remove any leftover soil. The stalks were allowed to air dry to evaporate off surface water and then placed in an oven at 65°C for about 2 days until a constant mass was obtained. The dried KS was then blended and sieved through a laboratory stainless steel test sieve to obtain the particles size of < 355 μm, and used throughout the experiment. The AO dye, molecular formula of $C_{17}H_{21}N_3$ and molar mass of 303.84 g mol^{-1}, was purchased from Sigma-Aldrich Corporation, USA, and used without further purification.

The KS:AO mixtures used in all the batch adsorption experiments were kept in the ratio of 1:500 (mass:volume) and shaken at 250 rpm on the Stuart SSL1 orbital shaker, UK, at room temperature, unless otherwise stated. Investigated parameters optimized were the time to reach equilibrium, effects of changes in pH and ionic strength, following the methods as described by Lim et al. [27]. Adsorption isotherm was carried out using AO dye concentrations ranging from 0 to 4,000 mg L^{-1} while kinetic studies were carried out using 100 mg L^{-1} AO dye. Thermodynamic studies were carried out within the temperature range of 298–343 K.

Measurements of the removal of AO dye were taken at its maximum wavelength of 460 nm using the Thermo Scientific Genesys 20 UV-Visible spectrophotometer, USA. EDT instruments GP353 ATC pH meter, UK, was used for all pH measurements. Functional group characterization of KS, before and after adsorption of AO dye, was determined with the Shimadzu Model IRPrestige-21 Fourier transform infrared spectroscopy (FTIR) spectrophotometer, Japan. Changes in surface morphology were recorded using Quanta 400, FEI, Scanning electron microscope (SEM, Czech Republic), while surface area and pore size were measured using Brunauer–Emmett–Teller (BET) apparatus (ASAP2460) Micromeritics, USA.

3. Results and discussion

3.1. Effect of contact time

Determination of contact time is crucial as it provides information on the time required for an adsorbate–adsorbent system to reach equilibrium. As seen from Fig. 2, the adsorption of AO dye using KS was very rapid within the first 30 min of the contact time, thereafter remaining more or less constant throughout the time range of investigation of 240 min. This can be attributed to the high dye concentration in the initial stage which provides the driving force for adsorption onto the freely available vacant sites on the adsorbent's surface, overcoming mass transfer resistance of the dye molecules between the aqueous and solid phases. Hence, the rest of the batch adsorption studies were carried out using 30 min contact time. Compared with commercial and laboratory grade activated carbon, as shown in Table 1, KS reaches equilibrium at a relatively short period, which is an advantage in wastewater application in terms of cost saving and efficiency.

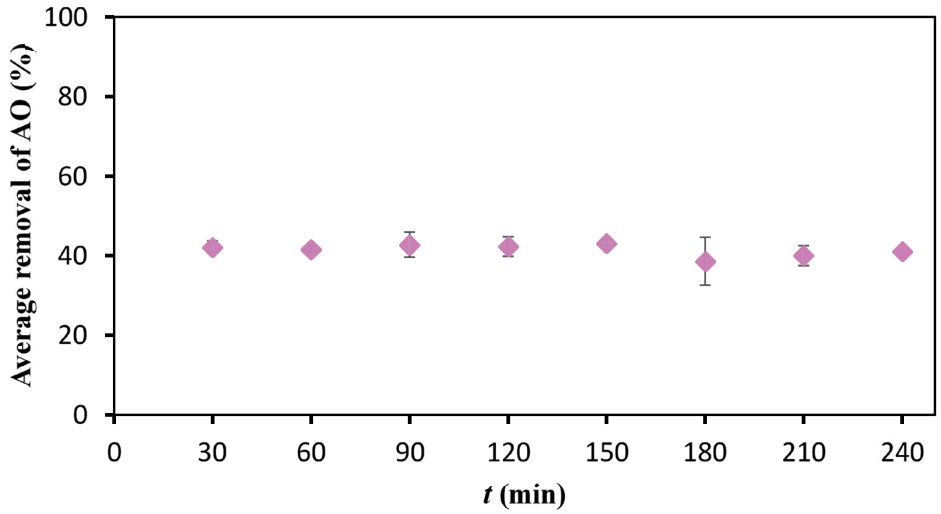

Fig. 2. Effect of contact time for the adsorption of AO by KS to reach plateau (mass of adsorbent = 0.050 g; volume of AO = 25.0 mL; concentration of AO = 100 mg L^{-1}).

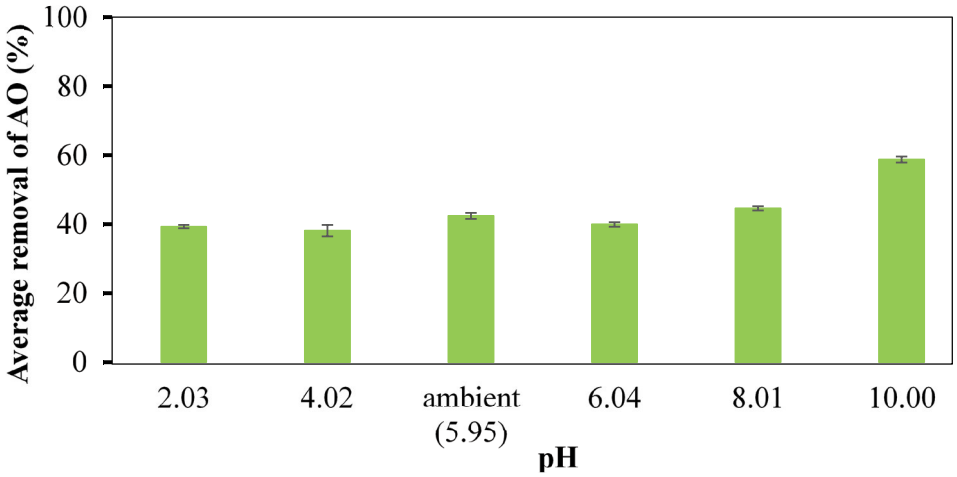

Fig. 3. Effect of medium pH on the adsorption of AO onto KS in different medium pH (mass of adsorbent = 0.050 g; volume of AO = 25.0 mL; concentration of AO = 100 mg L^{-1}).

Table 1
Comparison of contact time for various adsorbents to reach equilibrium with AO dye

Adsorbent	Time (min)	Reference
KS	30	This study
Bagasse fly ash	30	[28]
Commercial activated carbon	120	[28]
Laboratory grade activated carbon	120	[28]
Surface-modified mesoporous carbon	30	[29]

3.2. *Effect of pH on adsorption of AO by KS*

Generally, pH can affect the adsorption capacity of an adsorbent towards an adsorbate through protonation of the surface functional groups and/or the adsorbate. High concentration of H^+ ions could result in competition with the adsorbates for the vacant sites on the adsorbent's surface [30]. Many reported adsorbents are highly influenced by the change in medium pH, showing a great reduction in its removal ability at extreme pH [31,32]. It can be observed from Fig. 3 that KS is relatively unaffected by change in medium pH, especially under acidic condition unlike some reported adsorbents, such as carboxylated cellulose derivative [33]. Higher removal was observed at pH 10, which is in line with the point of zero charge (pH_{PZC}) of KS found to be at pH 7.43, as shown in Fig. 4. When pH > pH_{PZC}, deprotonation should result in the surface of KS to be predominantly negatively charged. AO being a cationic dye would, therefore, be more attracted to KS leading to increased adsorption. This is in line with the observed higher removal of AO by KS above pH_{pzc}. As for the rest of the pH, the removal was compatible with that

at the untreated (ambient) pH. Resilient of KS to change in medium pH is, therefore, an attractive and unusual feature since pH of wastewater usually differs depending on what pollutants are present and KS being able to uphold its adsorption capability over a range of pH will still be likely to maintain its adsorption towards AO dye. In this study, no adjustment of pH was made.

3.3. Effect of NaCl concentration on adsorption

Since contaminated water usually contains various chemicals including salts in different amounts, the presence of salts can affect an adsorbent's ability to adsorb an adsorbate. Many reports have shown that even a small concentration of salt can significantly reduce the amount of adsorbate being removed by an adsorbent. In this study, under various NaCl concentrations as shown in Fig. 5, KS showed a reduction in its adsorption capacity towards AO dye. This could be due to competition from the Na^+ ions with the cationic AO dye for the surface's active sites.

3.4. Adsorption isotherm and thermodynamic studies

Adsorption isotherm data obtained over a concentration range up to 4,000 mg L^{-1} AO dye concentration were fitted to five isotherm models, namely Langmuir [34], Freundlich [35], Redlich–Peterson (R–P) [36], Sips [37] and Temkin [38], whose equations are shown in Table 2. The first two models depict monolayer and multilayer adsorption, respectively, while the next two are three-parameter isotherm models with the Sips model being commonly known as the Langmuir–Freundlich model. The Temkin model is a two-parameter model, which describes the adsorbate–adsorbent relationship whereby interactions between them results in a linear decrease of heat of adsorption with increasing surface coverage and that the binding energies are uniformly distributed.

Five different error functions, namely average relative error (ARE), sum square error (SSE), sum of absolute errors (EABS), Marquardt's percent standard deviation (MPSD) and non-linear chi-square test (χ^2), were used to help in the evaluation of the best fit model for the adsorption process and their equations are shown in Table 3. The lower error

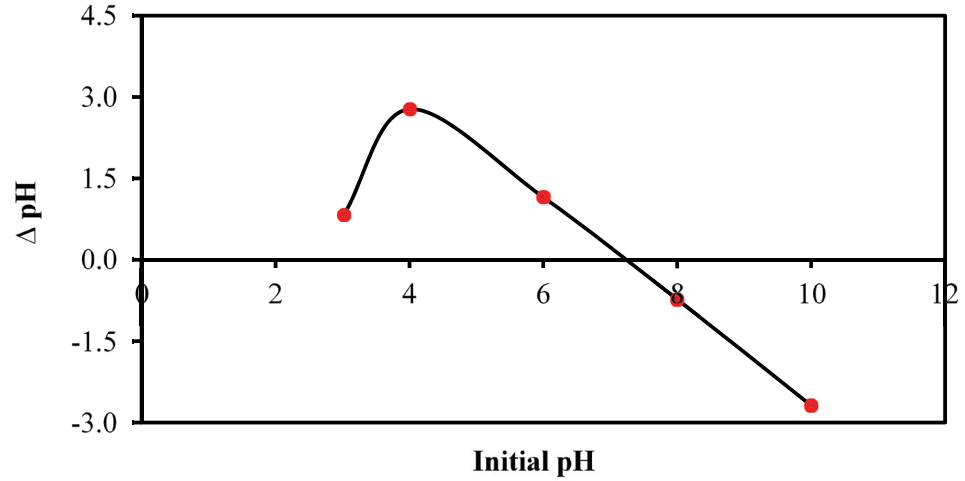

Fig. 4. Plot to determine the point of zero charge of KS (mass of adsorbent = 0.050 g; volume of AO = 25.0 mL).

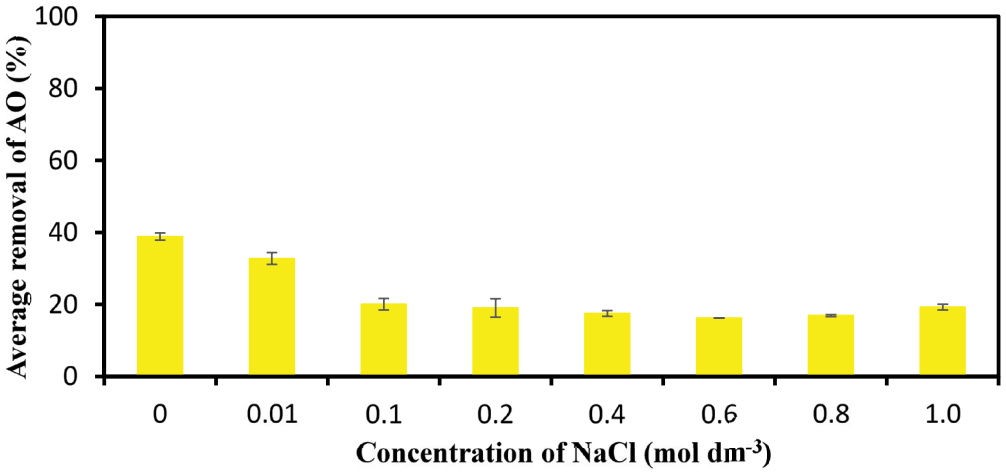

Fig. 5. Effect of ionic strength of NaCl (mass of adsorbent = 0.050 g; volume of AO = 25.0 mL; concentration of AO = 100 mg L^{-1}).

Table 2
Five isotherm models used and their corresponding linearized equations and plots

Isotherm model	Linearized equation	Plot
Langmuir	$\frac{C_e}{q_e}=\frac{1}{K_L q_{\max}}+\frac{C_e}{q_{\max}}$	$\frac{C_e}{q_e}$ vs. C_e
	C_e and q_e are the concentration and adsorption capacity at equilibrium, respectively; K_L is the Langmuir constant and $q_{\max}$ is the maximum adsorption capacity	
Freundlich	$\log q_e=\frac{1}{n}\log C_e+\log K_F$	$\log q_e$ vs. $\log C_e$
	K_F is the Freundlich constant indicative of adsorption capacity; n is related to the adsorption intensity	
Temkin	$q_e=\left(\frac{RT}{b_T}\right)\ln K_T+\left(\frac{RT}{b_T}\right)\ln C_e$	q_e vs. $\ln C_e$
	K_T is the Temkin constant; b_T is related to the heat of adsorption; R is the gas constant while T is the absolute temperature at 298 K	
Redlich–Peterson (R-P)	$\ln\left(\frac{K_R C_e}{q_e}-1\right)=n\ln C_e+\ln a_R$	$\ln\left(\frac{K_R C_e}{q_e}-1\right)$ vs. $\ln C_e$
	K_R and a_R are the R-P constants and n is the empirical parameter related to the adsorption intensity	
Sips	$\ln\left(\frac{q_e}{q_{\max}-q_e}\right)=\frac{1}{n}\ln C_e+\ln K_s$	$\ln\left(\frac{q_e}{q_{\max}-q_e}\right)$ vs. $\ln C_e$
	K_S is the Sips constant; n is the Sips exponent	

Table 3
Five error functions used in this study

Type of error functions	Abbreviation	Equations
Average relative error	ARE	$\frac{100}{n}\sum_{i=1}^{n}\left\lvert\frac{q_{e,\text{meas}}-q_{e,\text{calc}}}{q_{e,\text{meas}}}\right\rvert_i$
Sum square error	SSE	$\sum_{i=1}^{n}\left(q_{e,\text{calc}}-q_{e,\text{meas}}\right)_i^2$
Sum of absolute errors	EABS	$\sum_{i=1}^{n}\left\lvert q_{e,\text{meas}}-q_{e,\text{calc}}\right\rvert$
Marquardt's percent standard deviation	MPSD	$100\sqrt{\frac{1}{n-p}\sum_{i=1}^{n}\left(\frac{q_{e,\text{meas}}-q_{e,\text{calc}}}{q_{e,\text{meas}}}\right)_i^2}$
Non-linear chi-square test	χ^2	$\sum_{i=1}^{n}\frac{\left(q_{e,\text{meas}}-q_{e,\text{calc}}\right)^2}{q_{e,\text{meas}}}$

values would be an indication of a better fit to the experiment data.

The simulation plots shown in Fig. 6 clearly indicate the invalidity of the R-P model having the lowest R^2. Even though the Freundlich model having the second highest R^2 value (Table 4), its simulation plot is very much deviated from the experiment data thereby clearly indicating that it is an unsuitable model to describe the adsorption process. On the other

hand, the Temkin model can be eliminated as it showed high error values. Both the Sips and Langmuir models can be used to describe the adsorption process with the Sips isotherm model having higher R^2 (0.9615) as compared with the Langmuir model (0.9426) and overall smaller errors (Table 4). The maximum adsorption capacity (q_{max}) was found to be 303.83 mg g^{-1} based on the Sips model and monolayer adsorption using the Langmuir model led to a very close value of 299.76 mg g^{-1}.

According to the Langmuir isotherm, adsorption can be determined to be favourable or unfavourable by calculating R_L based on Eq. (1), as shown below. For the adsorption of AO onto KS, the R_L values lie between 0.14 and 0.98, indicating that the adsorption is a favourable process. This can be further confirmed from the Freundlich isotherm where $n > 1$, in this case $n = 1.367$, is indicative of a favourable adsorption process.

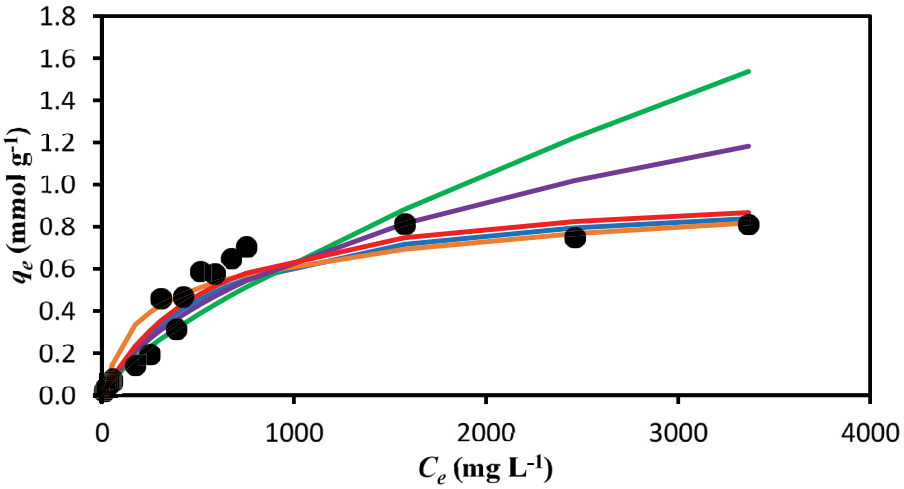

Fig. 6. Comparison of simulation plots of different types of isotherm models with experimental data such as Freundlich (——), R-P (——), Sips (——), Langmuir (——), Temkin (——) and experimental data (●) (mass of adsorbent = 0.050 g; volume of AO = 25.0 mL; concentration of AO = 0 to 4,000 mg L^{-1}).

Table 4
Values from the five isotherm models and five error functions used for the adsorption of AO on KS

Isotherm model and parameters	Values	ARE	SSE	EABS	MPSD	χ^2
Langmuir		18.41	0.12	1.16	24.09	0.38
q_{max} (mmol g^{-1})	0.987					
K_L (L $mmol^{-1}$)	0.002					
R^2	0.9426					
Freundlich		22.33	0.94	2.41	32.32	0.88
K_F (mmol g^{-1} (L $mmol^{-1})^{1/n}$)	0.004					
n	1.367					
R^2	0.9510					
Temkin		98.64	0.20	1.65	204.94	6.67
K_T (L $mmol^{-1}$)	0.044					
b_T (kJ mol^{-1})	15.182					
R^2	0.8911					
Redlich–Peterson		20.01	0.33	1.68	26.34	0.51
K_R (L g^{-1})	0.002					
α	0.651					
a_R (L $mmol^{-1}$)	0.024					
R^2	0.8026					
Sips		18.94	0.10	1.09	26.34	0.31
q_{max} (mmol g^{-1})	1.000					
K_S (L $mmol^{-1}$)	0.001					
n	0.967					
R^2	0.9615					

$$R_L = \frac{1}{1 + K_L C_0} \quad (1)$$

When compared with some reported adsorbents as shown in Table 5, KS was found to be superior in terms of adsorption towards AO dye to many, including activated carbon and other synthesized or modified adsorbents. Therefore, it was not necessary to carry out any surface modification attempts except that KS was dried via oven heating at 65°C. Some adsorbents, such as tannins, derived from *Caesalpinia spinosa* (Tara) and *Castanea sativa* (Chestnut) were found to be ineffective in removing AO dye [39]. Ghaedi et al. [40] reported an enhancement in AO dye removal with reduction in adsorption time when copper sulfide nanoparticle was ultrasonicated.

Thermodynamic studies play an important role in that the data obtained can contribute to the proper, efficient design and application of wastewater treatment. In this study, apart from room temperature, the adsorption of AO by KS was also investigated at four different temperatures (Fig. 7).

The changes in Gibbs free energy ($\Delta G°$), enthalpy ($\Delta H°$) and entropy ($\Delta S°$) were evaluated using Eqs. (2)–(5) by plotting the Van't Hoff relationship as shown in Fig. 8.

Table 5
Maximum adsorption capacity (q_{max}) of AO dye by various reported adsorbents

Adsorbent	q_{max} (mg g^{-1})	Reference
KS	303.8 (Sips) 299.8 (Langmuir)	This study
Bagasse fly ash	31.2	[28]
Commercial activated carbon	1.5	[28]
Laboratory grade activated carbon	12.6	[28]
Activated carbon	16.7	[41]
Psidium guajava leaves	7.8	[41]
ZnS:Cu nanoparticles on activated carbon	183.2	[42]
Surface-modified mesoporous carbon	172.0	[29]
Halloysite nanotubes ($Al_2Si_2O_5(OH)_4 \cdot 2H_2O$)	64.0	[43]
Natural untreated clay	833.3	[44]
Biopolymer poly(γ-glutamic acid)	277.3	[45]
Fertilizer plant waste carbon	246.3	[46]
ZnO:Cr nanoparticles–loaded activated carbon	211.6	[47]
Ultrasound-assisted ZnS:Cu nanoparticles on activated carbon	94.2	[48]
Oxidized cellulose	1,223.3	[49]
Oxidized sugarcane bagasse	682.8	[49]
Nanohydrogel	337.8	[50]
MCM-41 mesoporous silica nanoparticles	62.5	[51]
Sesame leaf	249.2	[52]

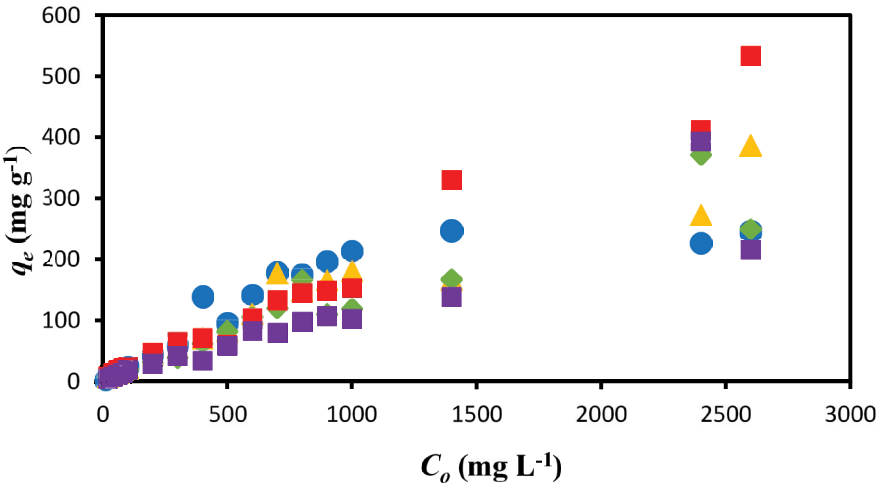

Fig. 7. Adsorption isotherms for the removal of AO by KS at 298 (●), 313 (▲), 323 (◆), 333 (■) and 343 K (■).

$$\Delta G^\circ = \Delta H^\circ - T\Delta S^\circ \quad (2)$$

$$\Delta G^\circ = -RT\ln K \quad (3)$$

$$K = \frac{C_s}{C_e} \quad (4)$$

$$\ln K = \frac{\Delta S^\circ}{R} - \frac{\Delta H^\circ}{RT} \quad (5)$$

where T is the temperature in Kelvin (K), R is the gas constant (J mol^{-1} K^{-1}), K being the adsorption distribution coefficient, C_s is the adsorbed dye concentration at equilibrium (mg L^{-1}), and C_e is the remaining dye concentration in solution at equilibrium (mg L^{-1}).

Table 6 shows the thermodynamics parameters obtained. It can be deduced that the adsorption of AO dye onto KS was exothermic in nature with increasing orderliness as temperature increases as shown by the negative $\Delta H^\circ$and ΔS°, respectively. Negative ΔG° suggests that the adsorption of AO on KS takes place spontaneously and favourably, which is in agreement with R_L and n values shown from the Langmuir and Freundlich isotherm models, respectively.

3.5. Kinetic studies on the adsorption of AO by KS

Two kinetic models were used for the investigation of the adsorption of AO by KS. The Lagergren pseudo-first order [53] is based on the assumption that the adsorbate concentration is constant and adsorption energy is independent of surface coverage. Adsorption takes place on localized surface sites with no interactions with the adsorbed ions. The pseudo-second order kinetic model [54] has more or less the same assumptions as the pseudo-first order, with the exception that the adsorption follows the second rate order equation. It also assumes that the adsorption involves chemisorption. The linearized Lagergren pseudo-first order and pseudo-second order models are presented by Eqs. (6) and (7), respectively, as follows:

$$\log\left(q_e - q_t\right) = \log\left(q_e\right) - \frac{k_1}{2.303}t \quad (6)$$

$$\frac{t}{q_t} = \frac{1}{k_2 q_e^2} + \frac{1}{q_e}t \quad (7)$$

where k_1 and k_2 are the rate constants for the Lagergren pseudo-first and pseudo-second order models, respectively.

Based on the linear plots of the two models used, as shown in Fig. 9, kinetics data showed that the adsorption mechanism followed the pseudo-second order kinetics as shown by its high R^2 value very close to unity (> 0.998), while the R^2 value for Lagergren pseudo-first order is < 0.167. This is further confirmed by the overall low error values for the pseudo-second order model based on five different error functions (Table 7), as well as the agreement of simulated pseudo-second order plot with the experiment data as illustrated in Fig. 10. According to the experiment data, q_{expt} was 0.079 mmol g^{-1}, a value very close to that of pseudo-second order where q_{calc} was found to be 0.072 mmol g^{-1} whereas for pseudo-first order the q_{calc} was 0.008 mmol g^{-1}, which clearly deviated from the experiment value.

Table 6
Thermodynamics data for the adsorption of AO onto KS

Parameter	Temperature (K)				
	298	313	323	333	343
q_{max} (mg g^{-1})	297.9	453.5	376.7	548.0	365.0
ΔG° (kJ mol^{-1})	–15.51	–14.63	–14.43	–14.67	–14.68
ΔH° (kJ mol^{-1})	–20.50				
ΔS° (J mol^{-1} K^{-1})	–17.77				

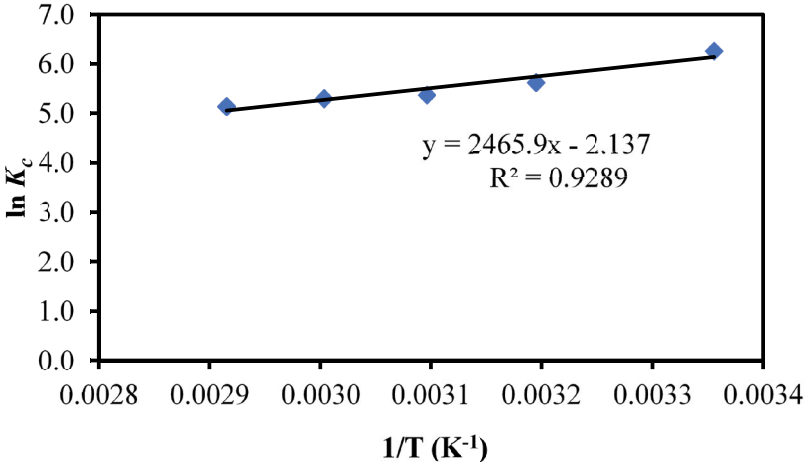

Fig. 8. Van't Hoff plot for the adsorption of AO onto KS (mass of adsorbent = 0.050 g; volume of AO = 25.0 mL).

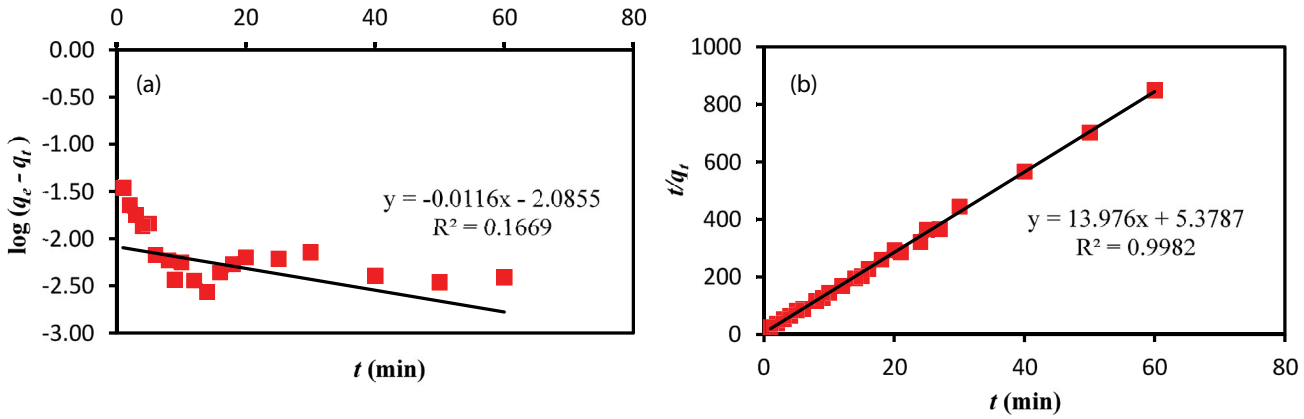

Fig. 9. Linear plots of the Lagergren pseudo-first order (a) and pseudo-second order (b) models for the adsorption of AO onto KS (mass of adsorbent = 0.050 g; volume of AO = 25.0 mL).

Table 7
Kinetics and error values of adsorption of AO dye on KS based on the pseudo-first and pseudo-second order models

Kinetics model	Parameter	ARE	SSE	EABS	MPSD	χ^2
Pseudo-first order		95.983	0.096	1.476	100.482	1.415
q_{expt} (mmol g^{-1})	0.079					
q_{calc} (mmol g^{-1})	0.008					
k_1 (min^{-1})	0.027					
Pseudo-second order		13.865	0.003	0.178	25.826	0.066
q_{expt} (mmol g^{-1})	0.079					
q_{calc} (mmol g^{-1})	0.072					
k_2 (g $mmol^{-1}$ min^{-1})	36.315					

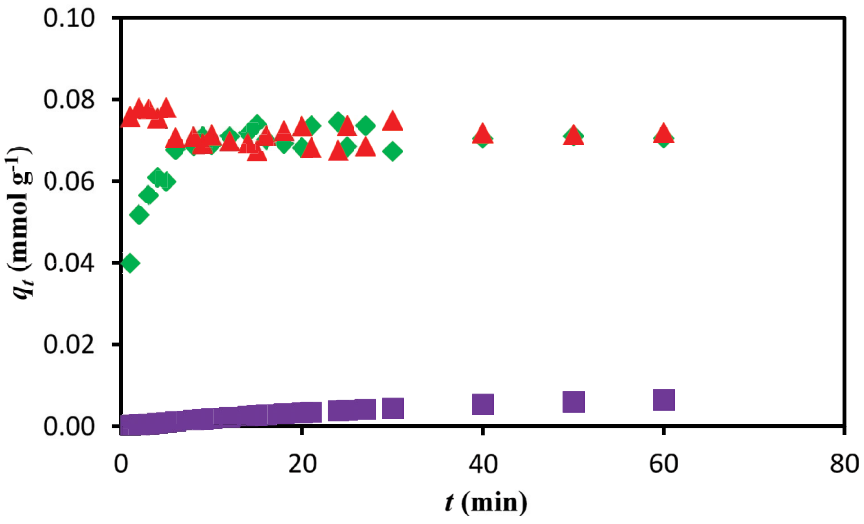

Fig. 10. Comparison of kinetics experimental data (◆) with simulation plots of the Lagergren pseudo-first (■), pseudo-second order (▲) models (mass of adsorbent = 0.050 g; volume of AO = 25.0 mL).

The above two kinetic models, that is, the Lagergren pseudo-first order and pseudo-second order models do not take into account the diffusional effects. Since it is possible for adsorbates to diffuse into adsorbents with porous surface, the Weber–Morris intraparticle diffusion model [55] was applied in this study to provide insight into the diffusion mechanism and its equation is as shown in Eq. (8), where k_i is the intraparticle rate constant, C is the intercept on the Y-axis of linear plot of q_t vs. $t^{1/2}$ and t is the time in min.

$$q_t = k_i t^{1/2} + C \quad (8)$$

In an adsorbent–adsorbate system, initial migration of the adsorbates will take place from the bulk solution to the surface of the adsorbent. This is then followed by diffusion of adsorbates into the pores of the adsorbent, and eventually an equilibrium is reached when migration of adsorbates from solution will cease to take place. Fig. 11 shows the different stages of mass transfer taking place during the adsorption of AO dye onto KS. According to the Weber–Morris model, pore diffusion is the rate determining step if q_t vs. $t^{1/2}$ shows a linear relationship passing through the origin; otherwise adsorption is controlled by film diffusion. The facts that q_t vs. $t^{1/2}$ does not pass the origin and that the occurrence of three linear portions indicate the complexity of the mass transfer process involving many modes of mass transfer including intra-particle diffusion to some extent.

3.6. Investigation of the regeneration and reusability of KS

To be economical in wastewater treatment application, a good and efficient adsorbent not only has to exhibit high adsorption ability towards an adsorbate, but it must also have the ability to be regenerated and reused. Not all adsorbents have the ability to be regenerated and reused. One such example is pectin extracted from durian rind where a reduction of approximately 70% was observed towards La^{3+} ions by the end of the fourth adsorption–desorption cycle [56]. Hence KS was investigated for its regeneration and reusability by treating the AO dye–loaded KS with acid, base and washing with distilled water. A control was also set up for comparison purpose. Of the three methods used, both acid and base treatment proved to be excellent ways of regenerating and reusing the adsorbent, as shown in Fig. 12. Treatment with base was the best method whereby the removal of AO was maintained above 80% over the five consecutive cycles. Simple washing and control experiment also showed that the KS was still able to adsorb AO dye even at cycle 5. Hence, it can be said that KS has the ability to be reused and therefore shows great potential as an adsorbent in real application in wastewater treatment.

3.7. Characterization of KS

Table 8 lists the surface area, pore size and pore volume of KS, before and after adsorption of AO dye, based on results obtained from BET analyses. It can be observed

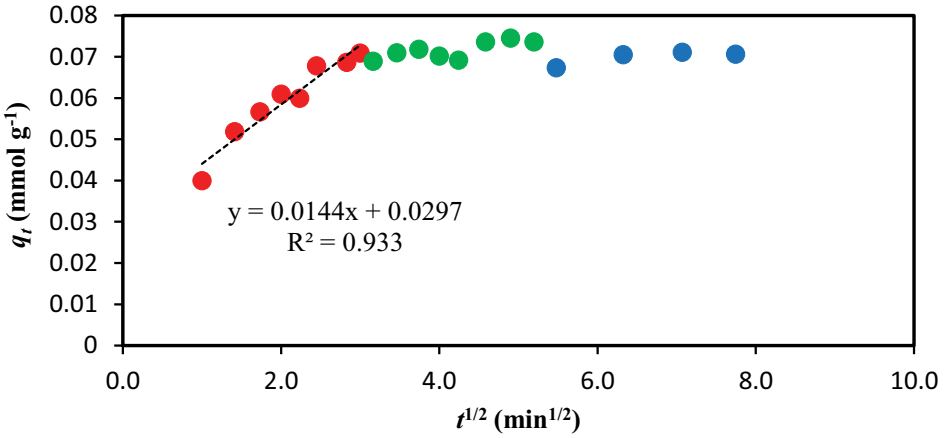

Fig. 11. Linear plot of Weber–Morris intraparticle diffusion model (mass of adsorbent = 0.050 g; volume of AO = 25.0 mL).

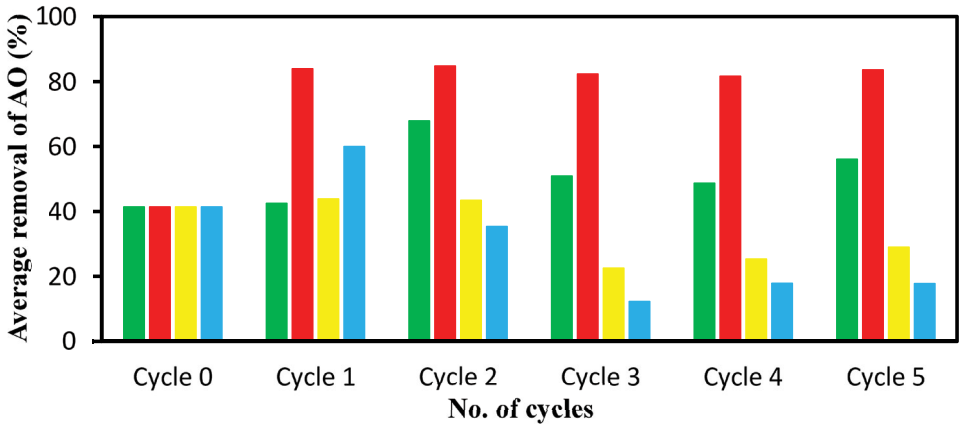

Fig. 12. Regeneration of KS using the treatment of acid (■), base (■), water (■) and control (■) for five consecutive cycles (mass of adsorbent = 0.050 g; concentration of AO = 100 mg L^{-1}).

that upon adsorption of AO dye, the pore size decreased significantly, indicating the coverage of active sites on the adsorbent's surface by the dye molecules. At the same time, the presence of dye molecules on the adsorbent's surface also resulted in an increase in the surface area of KS. This further supports the adsorption of the dye, where small dye molecules cover the surface of KS less evenly leaving many unadsorbed areas. This fact of incomplete surface coverage is further supported by by Fig. 13 where the SEM image after interaction of the dye does not show significant smoothening effect although the surface morphology of KS has changed when AO dye was adsorbed. Nevertheless, it is possible to have multilayers of AO dye on the KS surface on top of incomplete monolayer. Further, KS does not fluoresce when observed using fluorescent microscope imaging (Nikon Eclipse 50I pol), unlike the AO dye which is known to fluoresce as shown in Fig. 14. Confirmation of AO dye being successfully adsorbed onto KS can be clearly seen by the fluoresced KS-AO.

Table 8
BET results of KS before and after adsorption of AO dye

BET results	KS	KS-AO
Surface area ($m^2 g^{-1}$)	0.6584	3.4135
Pore volume ($cm^3 g^{-1}$)	0.001063	0.000168
Pore size (Å)	64.6106	1.9630

Fig. 15 shows the FTIR spectra of AO dye and KS before and after adsorption of AO. The functional groups present on the surface of KS that may be involved in the adsorption of AO dye molecules could be attributed to hydroxyl OH (3,405 cm^{-1}) and secondary amine groups (3,216 cm^{-1}) present

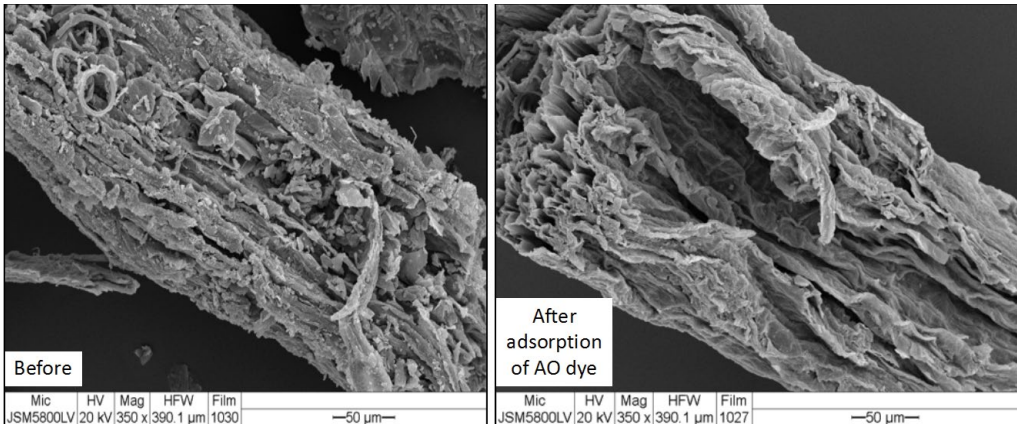

Fig. 13. Surface morphology of KS, before and after adsorption of AO dyes, analysed using SEM at 350 x magnification.

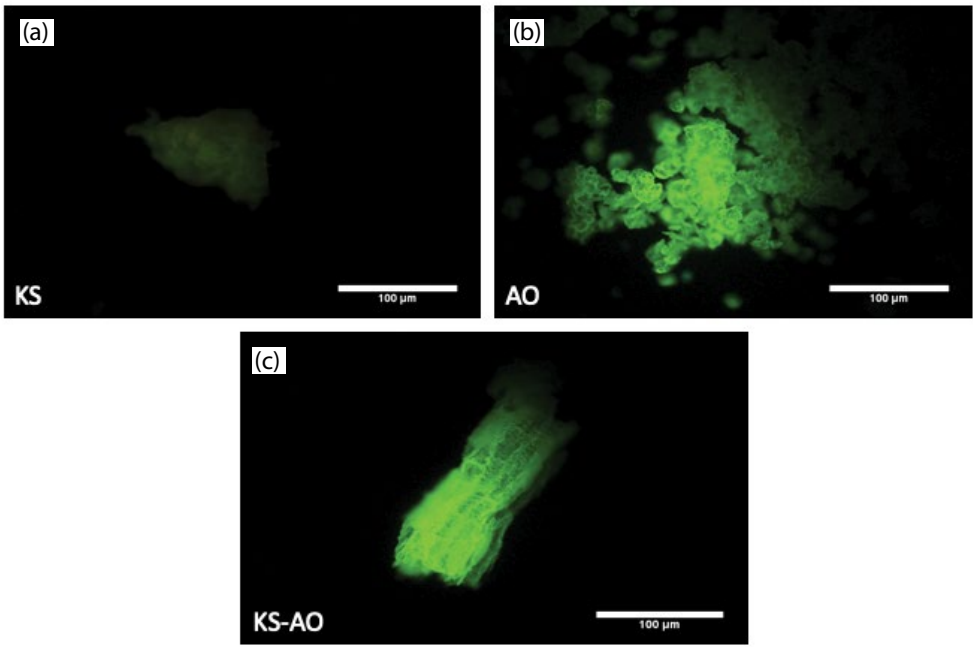

Fig. 14. Fluorescent images of (a) KS, (b) AO and (c) KS-AO.

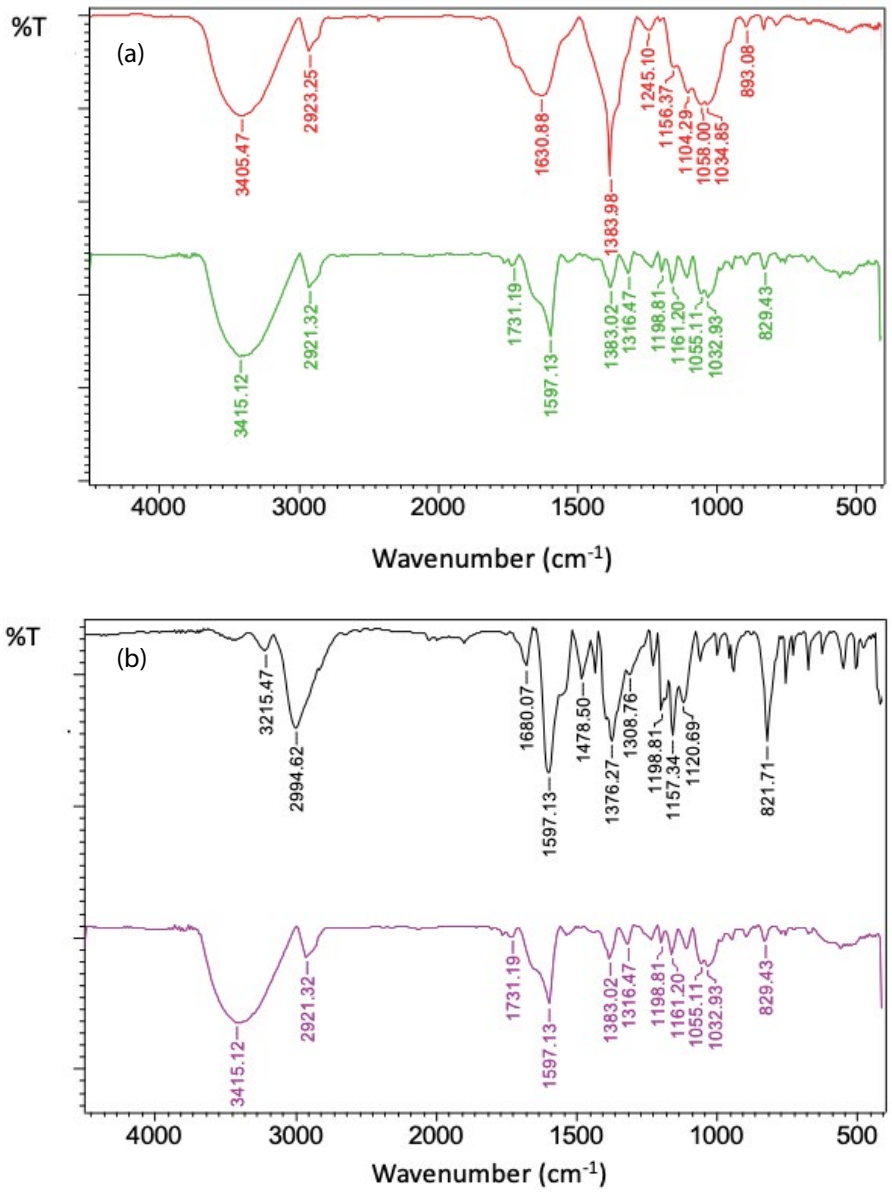

Fig. 15. FT-IR spectra of (a) KS (red) and KS-loaded with AO (green) and (b) AO (black) and KS-loaded with AO (purple).

in both KS and AO, respectively, which upon adsorption were both shifted. Other functional groups which may be involved include the imine group on AO at 1,681 cm^{-1} and also the para-substituted benzene out of plane of AO dye at 822 cm^{-1} which was shifted to 829 cm^{-1}. The of C=C aromatic rings of AO dye at 1,597 cm^{-1} was also detected in KS after dye treatment, confirming once again that AO was successfully adsorbed onto KS.

4. Conclusion

With its high q_{max} when compared with many reported adsorbents and being readily available in abundance throughout the year, *Ipomoea aquatica*, therefore, is a potential candidate as a low-cost adsorbent for the removal of AO dye. Not only does the adsorbent–adsorbate system took a very short time to reach equilibrium, its resilience to be affected in various medium pH, while at the same time maintaining good adsorption capacity, offers another attractive aspect as a good adsorbent to be considered and utilized in wastewater treatment. On top of that, KS has proven that it can be easily regenerated and reused, especially under acid or base treatment. This is an added feature since reusability and ease of regeneration are important features in adsorption work. Further enhancement of its q_{max} could be possible through surface modification.

Acknowledgements

The authors would like to thank the Government of Brunei Darussalam and Universiti Brunei Darussalam for their continuous support.

References

[1] L. Zhou, H. Zhou, Y. Hu, S. Yan, J. Yang, Adsorption removal of cationic dyes from aqueous solutions using ceramic adsorbents prepared from industrial waste coal gangue, J. Environ. Manage., 234 (2019) 245–252.

[2] L.B.L. Lim, N. Priyantha, Y. Lu, N.A.H.M. Zaidi, Effective removal of methyl violet dye using pomelo leaves as a new low-cost adsorbent, Desal. Wat. Treat., 110 (2018) 264–274.

[3] S.N. Jain, P.R. Gogate, Efficient removal of acid green 25 dye from wastewater using activated prunus dulcis as biosorbent: batch and column studies, J. Environ. Manage., 210 (2018) 226–238.

[4] R. Rehman, S. Farooq, T. Mahmud, Use of agro-waste musa acuminata and solanum tuberosum peels for economical sorptive removal of emerald green dye in ecofriendly way, J. Clean. Prod., 206 (2019) 819–826.

[5] L.B.L. Lim, N. Priyantha, K.J. Mek, N.A.H.M. Zaidi, Potential use of momordica charantia (Bitter gourd) waste as a low-cost adsorbent to remove toxic crystal violet dye, Desal. Wat. Treat., 82 (2017) 121–130.

[6] S. Shakoor, A. Nasar, Utilization of cucumis sativus peel as an eco-friendly biosorbent for the confiscation of crystal violet dye from artificially contaminated wastewater, Anal. Chem. Lett., 9 (2019) 1–19.

[7] L.B.L. Lim, N. Priyantha, T. Zehra, W. Then, C.M. Chan, Adsorption of crystal violet dye from aqueous solution onto chemically treated *Artocarpus odoratissimus* skin: equilibrium, thermodynamics, and kinetics studies, Desal. Wat. Treat., 57 (2016) 10246–10260.

[8] N. Kumar Mondal, S. Kar, Potentiality of banana peel for removal of congo red dye from aqueous solution: isotherm, kinetics and thermodynamics studies, Appl. Water Sci., 8 (2018) 157.

[9] N. Priyantha, L.B.L. Lim, D.T.B. Tennakoon, M.K. Dahri, N.H. Mohd Mansor, H.I. Chieng, Breadfruit (*Artocarpus altilis*) waste for bioremediation of Cu(II) and Cd(II) ions from aqueous medium, Ceylon J. Sci., 17 (2013) 19–29.

[10] V. Kumar, V. Rehani, B.S. Kaith, S. Saruchi, Synthesis of a biodegradable interpenetrating polymer network of Av-cl-poly(AA-ipn-AAm) for malachite green dye removal: kinetics and thermodynamic studies, RSC Adv., 8 (2018) 41920–41937.

[11] G. Bayazıt, Ü.D. Gül, D. Ünal, Biosorption of acid red P-2BX by lichens as low-cost biosorbents, Int. J. Environ. Stud., 76 (2019) 608–615.

[12] H.I. Chieng, L.B.L. Lim, N. Priyantha, D.T.B. Tennakoon, Sorption characteristics of peat of Brunei Darussalam III: equilibrium and kinetics studies on adsorption of crystal violet (CV), Int. J. Earth Sci. Eng., 6 (2013) 791–801.

[13] T. Zehra, L.B.L. Lim, N. Priyantha, Characterization of peat samples collected from Brunei Darussalam and their evaluation as potential adsorbents for Cu(II) removal from aqueous solution, Desal. Wat. Treat., 57 (2016) 20889–20903.

[14] R.W. Sabnis, Handbook of Biological Dyes and Stains: Synthesis and Industrial Applications, John Wiley & Sons, Inc., 2010.

[15] K. Sherfudeen, S. Kaliannan, P. Dammalapati, Cow dung powder poisoning, Indian J. Crit. Care Med., 19 (2015) 684.

[16] M. Hisham, A. Vijayakumar, N. Rajesh, M.N. Sivakumar, Auramine-o and malachite green poisoning: rare and fatal, Indian J. Pharm. Pract., 6 (2013) 72–74.

[17] S. Dhadke, V. Dhadke, A. Giram, Auramine-o (Synthetic Yellow Cow Dung Powder) poisoning: rare but fatal, J. Assoc. Physicians India, 65 (2017) 18–20.

[18] A. Muruganathan, M. Venkatesh, T. Ravikumar, S. Angayarkanni, P. Saravanan, Sopna Jothi, Yellow cow dung powder-(Auramine Poisoning)-Study of clinical profile, and statregies of management, IOSR J. Dent. Med. Sci., 16 (2017) 54–59.

[19] A. Martelli, G.B. Campart, R. Canonero, R. Carrozzino, F. Mattioli, L. Robbiano, M. Cavanna, Evaluation of auramine genotoxicity in primary rat and human hepatocytes and in the intact rat, Mutat. Res., 414 (1998) 37–47.

[20] S. Parodi, L. Santi, P. Russo, A. Albini, D. Vecchio, M. Pala, D. Ottaggio, A. Carbone, DNA damage induced by auramine o in liver, kidney, and bone marrow of rats and mice, and in a human cell line (alkaline elution assay and SCE induction), J. Toxicol. Environ. Health, 9 (1982) 941–952.

[21] J.C. Tung, W.C. Huang, J.C. Yang, G.Y. Chen, C.C. Fan, Y.C. Chien, P.S. Lin, S.C. Candice Lung, W.C. Chang, O. Auramine, an incense smoke ingredient, promotes lung cancer malignancy, Environ. Toxicol., 32 (2017) 2379–2391.

[22] K.J. Umar, L.G. Hassan, S.M. Dangoggo, M.J. Ladan, Nutritional composition of water spinach (*Ipomoea aquatica* Forsk.) leaves, J. Appl. Sci., 7 (2007) 803–809.

[23] P.K. Singh, S.K. Tiwari, N. Rai, K. Rai, M. Singh, Antioxidant and phytochemical levels and their interrelation in stem and leaf extract of water spinach (*Ipomea aquatica*), Indian J. Agric. Sci., 86 (2016) 347–354.

[24] A. Weerasinghe, S. Ariyawnasa, R. Weerasooriya, Phyto-remediation potential of Ipomoea aquatica for Cr(VI) mitigation, Chemosphere, 70 (2008) 521–524.

[25] L. Bedabati Chanu, A. Gupta, Phytoremediation of lead using Ipomoea aquatica Forsk. in hydroponic solution, Chemosphere, 156 (2016) 407–411.

[26] J.C. Chen, K.S. Wang, H. Chen, C.Y. Lu, L.C. Huang, H.C. Li, T.H. Peng, S.H. Chang, Phytoremediation of Cr(III) by Ipomonea aquatica (water spinach) from water in the presence of EDTA and chloride: Effects of Cr speciation, Bioresour. Technol., 101 (2010) 3033–3039.

[27] L.B.L. Lim, N. Priyantha, H.I. Chieng, M.K. Dahri, *Artocarpus camansi* blanco (Breadnut) core as low-cost adsorbent for the removal of methylene blue: equilibrium, thermodynamics, and kinetics studies, Desal. Wat. Treat., 57 (2016) 5673–5685.

[28] I. Deo Mall, V.C. Srivastava, N.K. Agarwal, Adsorptive removal of auramine o: kinetic and equilibrium study, J. Hazard. Mater., 143 (2007) 386–395.

[29] J. Goscianska, M. Marciniak, R. Pietrzak, The effect of surface modification of mesoporous carbons on Auramine-O dye removal from water, Adsorption, 22 (2016) 531–540.

[30] M.K. Dahri, L.B.L. Lim, C.C. Mei, Cempedak durian as a potential biosorbent for the removal of brilliant green dye from aqueous solution: equilibrium, thermodynamics and kinetics studies, Environ. Monit. Assess., 187 (2015) 546.

[31] B. Naraghi, F. Zabihi, M.R. Narooie, M. Saeidi, H. Biglari, Removal of acid orange 7 dye from aqueous solutions by adsorption onto kenya tea pulps; granulated shape, Electron. Physician, 9 (2017) 4312–4321.

[32] N. Priyantha, L.B.L. Lim, M.K. Dahri, Dragon fruit skin as a potential biosorbent for the removal of methylene blue dye from aqueous solution, Int. Food Res. J., 22 (2015) 2141–2148.

[33] F. Simões Teodoro, M. Madonyk Cota Elias, G. Max Dias Ferreira, O. Fernando Herrera Adarme, R. Marcello Leal Savedra, M. Fabíola Siqueira, L. Henrique Mendes da Silva, L. Frédéric Gil, L. Vinícius Alves Gurgel, Synthesis and application of a new carboxylated cellulose derivative. Part III: removal of auramine-O and safranin-T from mono-and bi-component spiked aqueous solutions, J. Colloid Interface Sci., 512 (2018) 575–590.

[34] I. Langmuir, The adsorption of gases on plane surfaces of glass, mica and platinum, J. Am. Chem. Soc., 40 (1918) 1361–1403.

[35] H. Freundlich, Over the adsorption in the solution, J. Phys. Chem., 57 (1906) 385–470.

[36] O. Redlich, D.L. Peterson, A useful adsorption isotherm, J. Phys. Chem., 63 (1959) 1024.

[37] R. Sips, On the structure of a catalyst surface, J. Chem. Phys., 16 (1948) 490–495.

[38] M.J. Temkin, V. Pyzhev, Kinetics of ammonia synthesis on promoted iron catalysts, Acta Physiochim, 12 (1940) 217.

[39] J. Sánchez Martín, J. Beltrán Heredia, J. Gragera Carvajal, *Caesalpinia spinosa* and *Castanea sativa* tannins: a new source of biopolymers with adsorbent capacity. preliminary assessment on cationic dye removal, Ind. Crops Prod., 34 (2011) 1238–1240.

[40] M. Ghaedi, S. Khodadoust, H. Sadeghi, M.A. Khodadoust, R. Armand, A. Fatehi, Application of ultrasonic radiation for simultaneous removal of auramine O and safranine O by copper

sulfide nanoparticles: experimental design, Spectrochim. Acta Part A Mol. Biomol. Spectrosc., 136 (2015) 1069–1075.
[41] R.W. Gaikwad, S.A.M. Kinldy, Studies on auramine dye adsorption on psidium guava leaves, Korean J. Chem. Eng., 26 (2009) 102–107.
[42] A. Asfaram, M. Ghaedi, S. Agarwal, I. Tyagi, V.K. Gupta, Removal of basic dye Auramine-O by ZnS:Cu nanoparticles loaded on activated carbon: optimization of parameters using response surface methodology with central composite design, RSC Adv., 5 (2015) 18438–18450.
[43] N. Khatri, S. Tyagii, D. Rawtani, Removal of basic dyes auramine yellow and auramine O by halloysite nanotubes, Int. J. Environ. Waste Manage., 17 (2016) 44–59.
[44] A. Öztürk, E. Malkoc, Adsorptive potential of cationic basic yellow 2 (BY2) dye onto natural untreated clay (NUC) from aqueous phase: mass transfer analysis, kinetic and equilibrium profile, Appl. Surf. Sci., 299 (2014) 105–115.
[45] B. Stephen Inbaraj, J.T. Chien, G.H. Ho, J. Yang, B.H. Chen, Equilibrium and kinetic studies on sorption of basic dyes by a natural biopolymer poly(-glutamic acid), Biochem. Eng. J., 31 (2006) 204–215.
[46] I. Mall, V. Srivastava, G. Kumar, I. Mishra, Characterization and utilization of mesoporous fertilizer plant waste carbon for adsorptive removal of dyes from aqueous solution, Physicochem. Eng. Asp., 278 (2006) 175–187.
[47] M. Jamshidi, M. Ghaedi, K. Dashtian, S. Hajati, A.A. Bazrafshan, Sonochemical assisted hydrothermal synthesis of ZnO: Cr nanoparticles loaded activated carbon for simultaneous ultrasound-assisted adsorption of ternary toxic organic dye: derivative spectrophotometric, optimization, kinetic and isotherm study, Ultrason. Sonochem., 32 (2016) 119–131.
[48] A. Asfaram, M. Ghaedi, S. Hajati, M. Rezaeinejad, A. Goudarzi, K. Purkait, Rapid removal of auramine-o and methylene blue by ZnS:Cu nanoparticles loaded on activated carbon: a response surface methodology approach, J. Taiwan Inst. Chem. Eng., 53 (2015) 80–91.
[49] L.R. Martins, J.A.V. Rodrigues, O.F.H. Adarme, T.M.S. Melo, L.V.A. Gurgel, L.F. Gil, Optimization of cellulose and sugarcane bagasse oxidation: application for adsorptive removal of crystal violet and auramine-o from aqueous solution, J. Colloid Interface Sci., 494 (2017) 223–241.
[50] V.P. Mahida, M.P. Patel, Removal of some most hazardous cationic dyes using novel poly (NIPAAm/AA/N-allylisatin) nanohydrogel, Arab. J. Chem., 9 (2016) 430–442.
[51] S.K. Hassaninejad Darzi, H.Z. Mousavi, M. Ebrahimpour, Biosorption of acridine orange and auramine o dyes onto MCM-41 mesoporous silica nanoparticles using high-accuracy UV–Vis partial least squares regression, J. Mol. Liq., 248 (2017) 990–1002.
[52] J. Liu, L.E. Liu, F. Yu, X. Han, H. Zhang, B. Zhang, Removal of auramine o from aqueous solution using sesame leaf: adsorption isotherm and kinetic studies, Asian J. Chem., 25 (2013) 1991–1998.
[53] S. Lagergren, About the theory of so-called adsorption of soluble substances, K. Sven. Vetenskapsakad. Handl., 24 (1898) 1–39.
[54] Y.S. Ho, G. McKay, Sorption of dye from aqueous solution by peat, Chem. Eng. J., 70 (1998) 115–124.
[55] W. Weber, J. Morris, Kinetics of adsorption on carbon from solution, J. Sanit. Eng. Div., 89 (1963) 31–60.
[56] E. Kusrini, W. Wicaksono, C. Gunawan, N.Z.A. Daud, A. Usman, Kinetics, mechanism, and thermodynamics of lanthanum adsorption on pectin extracted from durian rind, J. Environ. Chem. Eng., 6 (2018) 6580–6588.